Analytic scaling functions applicable to dispersion measurements in percolative metal-insulator systems

D. S. McLachlan, W. D. Heiss, C. Chiteme, and Junjie Wu
Department of Physics, University of the Witwatersrand, PO Wits 2050, Johannesburg, South Africa
(Received 15 June 1998)

Scaling functions, $F_+(\omega/\omega_c^+)$ and $F_-(\omega/\omega_c^-)$ for $\phi>\phi_c$ and $\phi<\phi_c$, respectively, are derived from an equation for the complex conductivity of binary conductor-insulator composites. It is shown that the real and imaginary parts of $F_\pm$ display most properties required for the percolation scaling functions. One difference is that, for $\omega/\omega_c<1$, Re $F_-(\omega/\omega_c)$ has an ω dependence of $(1+t)/t$ and not ω^2 as previously predicted, but never conclusively observed. Experimental results on a graphite–Boron nitride system are given, which are in reasonable agreement with the $\omega^{(1+t)/t}$ behavior for Re F_-. Anomalies in the real dielectric constant just above ϕ_c are also discussed. [S0163-1829(98)07443-8]

I. INTRODUCTION

The ac and dc conductivities of resistor and resistor-capacitor (RC) networks and continuum conductor-insulator composites have been extensively studied for many years. In systems where there is a very sharp change (metal-insulator transition or MIT) in the dc conductivity at a critical volume fraction or percolation threshold denoted by ϕ_c, the most successful model, for both the dc and ac properties, has proved to be percolation theory. Early work concentrated on the dc properties, but since it was realized [1–6] that the percolation threshold is a critical point, and that the percolation equations could be arrived at from a scaling relation, several papers, which are referenced and discussed in a previous paper,[7] reporting experimental results on the ac conductivity have appeared. Review articles, containing the theory and some experimental results, on the complex ac conductivity and other properties of binary metal-insulator systems include Refs. 8–10.

In another paper, extensive dc conductivity and low frequency dielectric constant results on systems based on graphite (G) and hexagonal boron nitride (BN), which have what are probably the cleanest and sharpest dc MIT's yet observed in a continuum system, have been reported.[11,12] These G-BN results were found to obey the percolation equations, as a function of volume fraction in Refs. 11, 12. In Ref. 7 it was shown that the experimental dispersion results, for samples with various volume fractions of G, can be scaled onto two curves that are consistent with previously measured percolation parameters;[11,12] one curve refers to the real conductivity above and the other to the imaginary conductivity (real dielectric constant) below the critical volume. Unfortunately, the parameters $\omega_c^\pm$ that had to be used to achieve this scaling were found to be different from those expected from the scaling models (RC lattice[8] and anomalous diffusion[13]), no matter whether the ω_c^+ and ω_c^- were calculated using the accepted universal parameters or the already reported dc conductivity and low-frequency dielectric results.[11,12] However, there is agreement between the critical exponents, characterizing the frequency dependence of the real conductivity when $\phi>\phi_c$ (where ϕ denotes the conducting volume fraction), the imaginary conductivity for $\phi<\phi_c$ and the exponents found from the previously reported dc and low frequency ac results.[11,12]

One measurable scaling function that did not agree with the previous power law predictions[8–10] was that for the loss component in the insulating region. As these results were somewhat controversial they were not discussed in Ref. 7. In the meantime further measurements have been made on one of the G-BN systems[11,12] and other systems, using a recently acquired dielectric spectrometer system that is able to measure far smaller dielectric loss parameters as well as loss and phase angles. Some of these results are presented in this paper.

The present paper introduces scaling functions that can depend on *complex* conductivities. They closely fit results of the medium conductance σ_M, in particular the frequency (ω) dependence of the first-order real part for $\phi>\phi_c$ and the first-order imaginary part for $\phi<\phi_c$ as was shown in Ref. 7. Most of the scaling power laws given in Refs. 8–10 are obtained; the range of parameters over which these functions can be expected to generate accurate scaling functions is derived. It is also shown that, while the second-order terms of the scaling functions have the exponents $t/(s+t)$ for $\phi\approx\phi_c$ and $\omega/\omega_c\gg1$ as given in Refs. 8–10, the second-order exponents for low frequencies and $\phi\gtrsim0$ or $\phi\lesssim1$ differ from those of Refs. 8–10. Experimental results for $\sigma_M(\omega,\phi)$ are presented that agree reasonably well with the exponents predicted by the introduced scaling functions, provided that the *complex* conductivities of the dielectric components of the continuum systems are taken into account. The measurements for $\sigma_M(\phi<\phi_c)$ in the G-BN systems are definitely not in accord with the ω^2 prediction given in Refs. 8–10.

A feature of the experimental results is that, where measurable, the real dielectric constant continues to increase with ϕ for $\phi>\phi_c$ and certainly does not decrease according to $(\phi-\phi_c)^{-s}$ as given in Refs. 8–10. However, this increase is qualitatively consistent with the expressions introduced in this paper. The effect is more clearly observed in carbon black-polyethylene compounds[14] and in three-dimensional systems where various conducting powders are distributed on the surfaces of large insulating grains.[15]

II. THEORY

The equation

$$\frac{(1-\phi)(\sigma_I^{1/s}-\sigma_M^{1/s})}{(\sigma_I^{1/s}+A\sigma_M^{1/s})}+\frac{\phi(\sigma_C^{1/t}-\sigma_M^{1/t})}{(\sigma_C^{1/t}+A\sigma_M^{1/t})}=0 \tag{1}$$

gives a *phenomenological* relationship between σ_C, σ_I, and σ_M, which are the conductivities of the conducting and insulating component and the mixture of the two components, respectively.[7,16] Results obtained from an earlier version[17] of Eq. (1) are reviewed in Ref. 18 and references therein, where the dc conductivities of some two phase systems are successfully modeled for $s=t$. The conducting volume fraction ϕ ranges between 0 and 1 with $\phi=0$ characterizing the pure insulator substance ($\sigma_M\equiv\sigma_I$) and $\phi=1$ the pure conductor substance ($\sigma_M\equiv\sigma_C$). The critical volume fraction, or percolation threshold, is denoted by ϕ_c, where a transition from an essentially insulating to an essentially conducting medium takes place. We use the notation $A=(1-\phi_c)/\phi_c$. For $s=t=1$ the equation is equivalent to the Bruggeman symmetric media equation.[18,19] The equation yields the two limits

$$|\sigma_C|\to\infty: \quad \sigma_M=\sigma_I\frac{\phi_c^s}{(\phi_c-\phi)^s}, \quad \phi<\phi_c \tag{2}$$

$$|\sigma_I|\to 0: \quad \sigma_M=\sigma_C\frac{(\phi-\phi_c)^t}{(1-\phi_c)^t}, \quad \phi>\phi_c, \tag{3}$$

which characterize the exponents s and t. Note that Eqs. (2) and (3) are the normalized percolation equations. For ac measurements, Refs. 8–10 have given equations for the case where σ_C is real and $\sigma_I=-i\omega\epsilon_0\epsilon_I$, which characterizes a lossless dielectric. However, we note that all three quantities σ_I, σ_C, and σ_M can in principle be complex numbers in Eq. (1). A solution for σ_M can be obtained after rewriting Eq. (1) using the variable $z=\sigma_M^{1/t}$, viz.,

$$Az^{1+\alpha}-z^{\alpha}(A\phi+\phi-1)\sigma_C^{1/t}-z(A-A\phi-\phi)\sigma_I^{\alpha/t} -(\sigma_I^{\alpha}\sigma_C)^{1/t}=0 \tag{4}$$

with $\alpha=t/s$. We note in passing that Eq. (4) has explicit solutions for $\alpha=1$, 2, and 3, while numerical solutions are easily obtained for larger integer values. Our interest is now focused on the question as to what extent the solution for σ_M can be used to obtain valid scaling functions.

The scaling conditions, which are based on those given in Refs. 8–10, read

$$\sigma_M=\begin{cases}\sigma_C\dfrac{(\phi_c-\phi)^t}{\phi_c^t}F_-(x_-), & \phi<\phi_c \quad (5)\\ \sigma_C\dfrac{(\phi-\phi_c)^t}{(1-\phi_c)^t}F_+(x_+), & \phi>\phi_c, \quad (6)\end{cases}$$

where the scaling functions $F_{\pm}(x_{\pm})$ depend on the scaling parameters

$$x_-=\frac{\sigma_I}{\sigma_C}\frac{\phi_c^{s+t}}{(\phi_c-\phi)^{s+t}}=-i\frac{\omega}{\omega_c^-}, \quad \phi<\phi_c \tag{7}$$

with

$$\omega_c^-=\frac{\sigma_C}{\epsilon_0\epsilon_I}\frac{(\phi_c-\phi)^{s+t}}{\phi_c^{s+t}},$$

and

$$x_+=\frac{\sigma_I}{\sigma_C}\frac{(1-\phi_c)^{s+t}}{(\phi-\phi_c)^{s+t}}=-i\frac{\omega}{\omega_c^+}, \quad \phi>\phi_c \tag{8}$$

with

$$\omega_c^+=\frac{\sigma_C}{\epsilon_0\epsilon_I}\frac{(\phi-\phi_c)^{s+t}}{(1-\phi_c)^{s+t}}.$$

The expressions involving $\omega^{\pm}$ assume specifically a purely real σ_C and imaginary σ_I. To ensure that curves drawn for $F_{\pm}$ fall on top of each other for different ϕ_c, the normalization employed in all the equations used in this paper differs somewhat from the one used in Refs. 8–10. Using the variable $u=F_-^{1/t}$ an equation is found for u by the substitution $z=u\sigma_C^{1/t}(\phi_c-\phi)/\phi_c$ in Eq. (4). It reads for $\phi<\phi_c$ as

$$Au^{1+\alpha}+u^{\alpha}-u\frac{(\phi_c-\phi)(1-\phi-\phi_c)}{\phi_c^2}x_-^{1/s}-x_-^{1/s}=0. \tag{9}$$

In a similar way, the substitution $z=u\sigma_C^{1/t}(\phi-\phi_c)/(1-\phi_c)$ leads to an equation for $F_+^{1/t}$ (again denoted by u) for $\phi>\phi_c$

$$Au^{1+\alpha}-Au^{\alpha}-u\frac{(\phi-\phi_c)(1-\phi-\phi_c)}{\phi_c(1-\phi_c)}x_+^{1/s}-x_+^{1/s}=0. \tag{10}$$

If the term linear in u of Eqs. (9) and (10) could be neglected, the scaling functions $F_{\pm}$ would manifestly depend only on the respective variables $x_{\pm}$. It is due to this term that scaling is invalidated to a certain degree by the solution for σ_M of Eq. (1). The range and extent to which this is the case are discussed below. An interesting aspect of Eqs. (9) and (10) is exact scaling at $\phi=\phi_c$ and $\phi=1-\phi_c$. Whether or not exact scaling for $\phi=1-\phi_c$ is merely a coincidence can only be revealed by appropriate experiments. We stress that all results obtained in this section are independent of whether the conductances and hence the scaling functions $F_{\pm}$ are genuinely complex or real.

Exact solutions of Eqs. (9) and (10) can be read off at the limit points of the concentration. At $\phi=0$, it is $u^{\alpha}=x_-^{1/s}$, i.e., $F_-\equiv x_-$ and at $\phi=1$, it is $u=1$, i.e., $F_+\equiv 1$. From these solutions, Eqs. (2) and (3) are obtained from Eqs. (5) and (6), respectively. In fact, the respective solutions are valid to high accuracy for $\phi>0$ and $\phi<1$ as long as $|x_{\pm}|\ll 1$ or for ϕ very close to either ϕ_c or $1-\phi_c$. Correction terms are given below.

For the opposite limit of the scaling parameters, i.e., $|x_{\pm}|\gg 1$, we obtain for the leading term at $\phi\approx\phi_c$ the solution $Au^{1+\alpha}=x^{1/s}$ from both equations, (9) and (10). This translates into

$$F_{\pm}=(x_{\pm})^{t/(s+t)}A^{-st/(s+t)}, \tag{11}$$

which gives

$$\sigma_M=\frac{\sigma_C}{A^{st/(s+t)}}\left(\frac{\sigma_I}{\sigma_C}\right)^{t/(s+t)} \quad \text{at} \quad \phi=\phi_c. \tag{12}$$

Note that Eq. (12) conveniently lends itself for complex values of σ_I and σ_C; in particular, if σ_I is purely imaginary and σ_C real one obtains

$$\text{Im } \sigma_M = -\frac{\sigma_C}{A^{st/(s+t)}} \left| \frac{\omega\epsilon_0\epsilon_I}{\sigma_C} \right|^{t/(s+t)} \sin\left(\frac{\pi t}{2(s+t)} \right), \tag{13}$$

$$\text{Re } \sigma_M = +\frac{\sigma_C}{A^{st/(s+t)}} \left| \frac{\omega\epsilon_0\epsilon_I}{\sigma_C} \right|^{t/(s+t)} \cos\left(\frac{\pi t}{2(s+t)} \right). \tag{14}$$

From Eq. (11) it follows that the slope of the real and imaginary part of $\ln(F_\pm)$ is $t/(t+s)$ when plotted against $\ln(x_\pm)$ for $|x_\pm| \gg 1$. Equations (13) and (14) show that, with $\sigma_I = -i\omega\epsilon_0\epsilon_I$, the frequency dependence of both real and imaginary σ_M is $\omega^{t/(s+t)}$. This dispersion law is given in Refs. 7–10. Experimental results validating this power law are found in Refs. 7, 12, 20–24. The loss angle $\delta = \arctan\{\pi t/[2(s+t)]\}$ implied by Eqs. (13) and (14) is also given in Ref. 8.

It is of physical interest to determine the correction terms of next order in Eqs. (2) and (3). Note that Eq. (2) yields a purely imaginary result for σ_M if σ_I is imaginary. However, a loss term should emerge for $\omega > 0$ when $\phi > 0$. This is obtained by expanding the solution of Eq. (9) for $\phi \gtrsim 0$. One finds for the scaling function

$$F_- = x_- - s\frac{\phi}{\phi_c^2} x_- \frac{x_-^{1/t}}{Ax_-^{1/t}+1} = \frac{\sigma_I}{\sigma_C}\left(1 + (s+t)\frac{\phi}{\phi_c} - s\frac{\phi}{\phi_c^2}\frac{(\sigma_I/\sigma_C)^{1/t}}{A(\sigma_I/\sigma_C)^{1/t}+1} \right), \tag{15}$$

which can be used for real or complex σ_I or σ_C. Combining Eq. (15) with Eq. (5) one obtains for small ϕ/ϕ_c, as expected, both an enhanced dielectric loss term $\text{Re } \sigma_I(1 + s\phi/\phi_c)$ and a composite loss term. Taking specifically σ_I purely imaginary and σ_C real, the composite loss term reads explicitly up to terms linear in ϕ/ϕ_c

$$\text{Re } \sigma_M = s\sigma_C \frac{\phi}{\phi_c^2} \frac{|\sigma_I/\sigma_C|^{(1+t)/t}\sin(\pi/2t)}{A|\sigma_I/\sigma_C|^{2/t} + 2A|\sigma_I/\sigma_C|^{1/t}\cos(\pi/2t) + 1}. \tag{16}$$

An important consequence of Eq. (16) is the small frequency behavior of the loss term (recall $\sigma_I = -i\omega\epsilon_0\epsilon_I$), which implies

$$\text{Re } \sigma_M \sim \omega^{(1+t)/t}, \tag{17}$$

which differs from the ω^2 behavior predicted by the expansions used for F_- in Refs. 8–10. We note that these expansions assume analytic behavior for σ_M around $\omega = 0$, which is in contrast to our findings; also we obtain a loss term that vanishes for $\phi \to 0$, which is not the case for the expressions in Refs. 8–10. The following section presents experimental results that appear to confirm the power law expressed by Eq. (17).

By similar means we obtain the first order correction term in the vicinity of $\phi \lesssim 1$, which reads

$$F_+ = 1 + t\frac{1-\phi}{\phi_c(1-\phi_c)}\frac{x_+^{1/s}}{A+x_+^{1/s}} = 1 + t\frac{1-\phi}{\phi_c(1-\phi_c)}\frac{(\sigma_I/\sigma_C)^{1/s}}{A+(\sigma_I/\sigma_C)^{1/s}}. \tag{18}$$

Note that this term implies not only a correction to the real part of σ_M in Eq. (3) but also a switching on of an imaginary part for complex σ_I. For purely imaginary σ_I this is

$$\text{Im } \sigma_M = -t\frac{1-\phi}{\phi_c(1-\phi_c)}\sigma_C \times \frac{|\sigma_I/\sigma_C|^{1/s}\sin(\pi/2s)}{A^2 + 2A|\sigma_I/\sigma_C|^{1/s}\cos(\pi/2s) + |\sigma_I/\sigma_C|^{2/s}} \tag{19}$$

which implies in this limit, for $\sigma_I = -i\omega\epsilon_0\epsilon_I$, that $\text{Im } \sigma_M \sim \omega^{1/s}$.

So far, we have concentrated on regions where scaling is obeyed by the solution of Eq. (1) either exactly or to high accuracy, that is, for $0 \leqslant \phi < \phi_c$ and $\phi_c < \phi \leqslant 1$, if $|x_\pm| \ll 1$, and for $\phi \approx \phi_c$, if $|x_\pm| \gg 1$. There is an intermediate region $|x_\pm| \sim 1$, where the linear term in u of Eqs. (9) and (10) invalidates the sole dependence of $F_\pm$ on $x_\pm$ except for $\phi = \phi_c$ or $\phi = 1 - \phi_c$. In fact, it can be shown that, as long as the inequality

$$\frac{\omega}{\omega_0} < \frac{\phi_c}{1-2\phi_c} \quad \text{with} \quad \omega_0 = \left| \frac{\sigma_C}{\epsilon_0\epsilon_I} \right| \tag{20}$$

is obeyed, the linear term of Eqs. (9) and (10) is immaterial and scaling prevails. As a consequence, the leading behavior of $F_\pm$, for $x_\pm \gg 1$, is governed by the power law $x_\pm^{t/(t+s)}$ only up to the frequency that obeys the inequality (20), for larger frequencies $F_\pm$ becomes a linear function of $x_\pm$. Note, however, that the right-hand side of Eq. (20) depends on ϕ_c in such a way that scaling is expected to be invalidated only for small values of ϕ_c and sufficiently large values of ω. In turn, for $\phi_c > 1/3$ the right-hand side of Eq. (20) is larger than unity, and for $\phi_c \to 1/2$ no bound on ω prevails. (Note that $\phi_c = 1/3$ is the Bruggeman value for spheres in three dimensions and $\phi_c = 1/2$ for discs in two dimensions.[18,19]) As a consequence, there should be no discernible deviations from scaling for $\phi_c > 1/3$. To what extent these results are physically valid can only be assessed by experiment. No experiments in this region appear to exist and the situation is complicated by the fact that σ_C and σ_I depend on ω when ω becomes sufficiently large.

In Fig. 1 we illustrate the behavior of the real and imaginary parts of $F_\pm(x_\pm)$ for $s = 1$, $t = 2$ and $\phi = \phi_c = 0.16$, that is for the situation where scaling holds exactly. As discussed above, deviations are marginal when ϕ is near to ϕ_c and become noticeable only when the inequality (20) is appreciably invalidated. Note the equal slopes for large $x_\pm$ of all four curves in accordance with Eqs. (13) and (14). Also, since $t > s$, the imaginary parts are larger than the real parts; for $s = t$ all four curves would coincide asymptotically. For $s > t$ the real parts would be larger than the imaginary parts but no such system has been observed or predicted.

We interpret the dependence on σ_I/σ_C of the percolation loss term as predicted by Eqs. (15)–(17) as follows: Con-

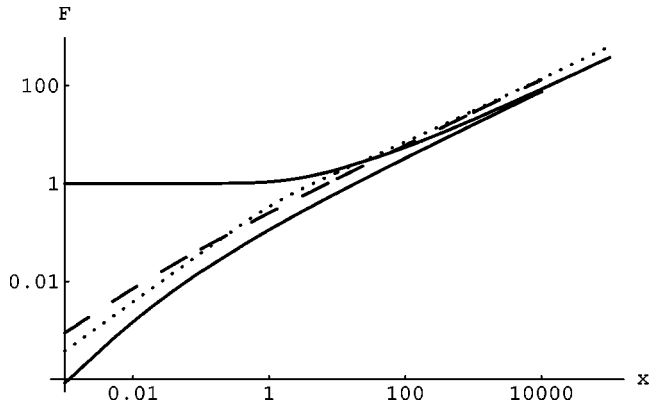

FIG. 1. Plots of F_+ and F_- against $x_+(\omega/\omega_c^+)$ and $x_-(\omega/\omega_c^-)$, respectively. The parameters used are $\phi \approx \phi_c = 0.16, s = 1$, and $t = 2$. As $\phi \approx \phi_c$ the values used for σ_C must be accordingly large to yield a finite $\omega_c^{\pm}$. The upper solid curve is Re F_+ and the lower one Re F_- (the second order dielectric loss term). The dashed line is Im F_- (the first-order term below ϕ_c), and the dotted line is Im F_+. Note how this term rises above Im F_- in the region where $x_\pm$ is between 1 and 100.

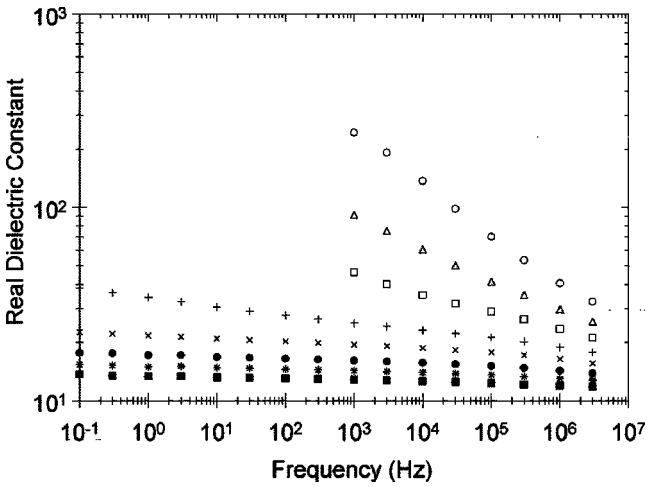

FIG. 2. A plot of the real part of the dielectric constant against frequency for a 55%-45% G-BN powder on a log-log scale for various values of ϕ [$\phi = 0.1309$ (open circles), 0.1290 (triangles), 0.1272 (open squares), 0.1236 (plus), 0.1219 (crosses), 0.1203 (dots), 0.1187 (asterisks), 0.1171 (solid squares)]. These are relative volume fractions, as the absolute error is about ± 0.001.

sider a three-dimensional lattice, with ideal capacitors on nearly all the bonds but with a small number of randomly distributed resistors embedded in the capacitor matrix, either as isolated components or as small clusters, and choose $C\omega < 1/R$. If a voltage is applied to two opposite faces of the lattice, the displacement current in the lattice is determined almost entirely by the capacitors. Therefore, as the current in the resistors is evoked by a ''fixed current source,'' which is determined by the value of $1/(C\omega)$, the dissipation is proportional to I^2R, i.e., the larger R the more power is dissipated. This argument can be extended to continuum systems, which qualitatively explains the dependence on σ_I/σ_C in Eq. (15). The presence of the exponent t, which determines the rate of increase of the conductivity beyond ϕ_c, would therefore appear to have a role in the formation of the conducting clusters, which determine the dissipation below ϕ_c. However, below ϕ_c, the behavior of the complex effective conductivity is dominated by the imaginary component, which is primarily determined by the interconnectivity of the insulating medium, or more specifically its ability of keeping the clusters of the conducting medium disconnected below ϕ_c, which in turn is characterized by the exponent s.

We note that the treatment given in Refs. 8–10 has no t or s dependence for $x_- < 1$ or $x_+ < 1$, respectively. However, our Eqs. (15) and (18), which are based upon Eqs. (9) and (10), indicate that the exponent t, which characterizes the formation of the conducting backbone, continues to play a role for $\phi < \phi_c$; similarly, the real dielectric constant is not independent of s for $\phi > \phi_c$.

III. EXPERIMENTAL METHOD

The percolation system[7,11,12] that best exhibits the $(1+t)/t$ behavior is a lightly poured powder of 55% graphite 45% boron nitride, which is compressed, expelling air, in a capacitive cell through the percolation threshold. As the percolation threshold is at 0.124 (volume fraction of G), the insulator at and around this point consists of 11.4% BN and 88.6% dry air, which obviously has a Re ϵ close to one and a very low Im ϵ term. The dissipation in more compacted systems, such as compressed pellets of G-BN (Ref. 7) or polyethylene-carbon black,[14] would appear to be dominated by the dissipation in the dielectric component.

As the constructions of the cells and experimental procedures for the G-BN powder have been adequately described for the dc and low-frequency ac measurements in Refs. 11 and 12 as well as the dispersion measurements [$\sigma_M(\omega)$ for fixed ϕ] in Refs. 7 and 12, they will not be repeated here. Some experimental results are presented, which are obtained by tumbling various conducting powders with larger wax coated insulating grains. The conductor coated grains are then compressed into disks.[15]

The measurements presented here are the results of the real and imaginary parts of the conductivity between 10^{-1} and 3.10^6 Hz, obtained using a newly acquired Novocontrol Dielectric Spectrometer. This instrument is able to measure far smaller loss components of the dielectric or insulating phase (equivalent to a resistor of $10^{18}\ \Omega$ at 10^{-1} Hz and $10^8\ \Omega$ at 10^5 Hz in parallel with a perfect capacitor) and had a better resolution of loss or phase angle (a maximum of tan δ of $>10^3$ and a minimum of $<10^{-3}$ can be measured) than the instruments used in Ref. 7 or measurements of a similar nature.[20–24]

IV. RESULTS AND DISCUSSION

The experimental results for Re ϵ and Re σ_M for the 55%G-45%BN powder as a function of frequency between 10^{-1} and 3×10^6 Hz are given in Figs. 2 and 3. The dispersion results for the three highest-lying curves in Fig. 3 are conducting samples ($\phi > \phi_c$) with dispersion free conductivities at low frequencies.[8–10] The dielectric constant of these three samples (upper curves in Fig. 2) show a strong dispersion, which should go from $s/(s+t) = 0.47/(0.47+4.8) \approx 0.09$ at ϕ_c to $1/s \approx 2$ near to $\phi = 1$. The observed values range from 0.1 to 0.33. The dielectric constant for the

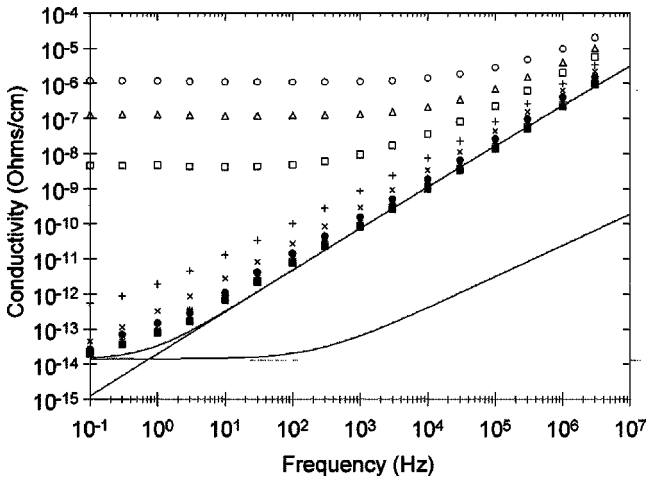

FIG. 3. A plot of the real part of the conductivity against frequency for a 55%-45% G-BN powder on a log log scale for various values of ϕ [$\phi=0.1309$ (open circles), 0.1290 (triangles), 0.1272 (open squares), 0.1236 (plus), 0.1219 (crosses), 0.1203 (dots), 0.1187 (asterisks), 0.1171 (solid squares)]. These are relative volume fractions as the absolute error is about ± 0.001.

conducting samples ($\phi > \phi_c$) will be further discussed below.

The sample marked by plus signs in Fig. 3 ($\phi - \phi_c = -0.0004 \pm 0.001$) is actually metallic, as its conductivity breaks away from a constant slope at sufficiently low frequencies, as predicted for metallic samples in this paper and Refs. 8–10. Note too that the larger exponent 0.15 for the higher frequencies shown by this sample in Fig. 2 also indicates that it is not an insulator ($x_- < 1$). When compared to the results in Fig. 1 in Ref. 7, this observation illustrates the necessity of making measurements at lower frequencies than previously done in any experiments of this nature.

In Fig. 2, the exponent of Re ϵ drops form -0.10 to -0.02 for the last four samples. While, from the results given in Ref. 7, a dispersion exponent of -0.10 could indicate a sample still in the $x_- > 1$ region, the fact that the sum of the absolute values of the exponents for the dispersion in Re ϵ and Re σ_M are greater than 1, precludes this possibility.[7–10] This, combined with the ever decreasing magnitude of the Re ϵ exponents, going down to 0.02 from the lowest-lying curve, allows us to conclude that these four samples lie in the dielectric or $x_- < 1$ region. Note that the lowest measured values for $s/(s+t)$ recorded in the literature[7,19–23] are 0.07 for 50%G-50%BN and 0.10 for 55%G-45%BN.[7]

Based on the arguments given above, the four lowest-lying plots of the conductivity against frequency in Fig. 3 are the conductivities for samples in the insulating or dielectric state ($x_- < 1$). There is a very slight upward curvature of the results between 10 and 3×10^6 Hz, but the mean slopes in this region are 1.06 and 1.09. The slope decreases below 3Hz. According to Eq. (15) the conductivity is made up of both a dielectric and percolation loss term, the relative contributions of which must now be examined.

In order to evaluate Eqs. (15), (16), (18), and (19), an expression for σ_I is required. Unfortunately the loss term in the boron nitride–air system is too small to measure directly on the dielectric spectrometer, which also meant that the percolation parameters for this system could not be measured directly. Therefore, the complex conductivity of boron nitride–air mixture had to be calculated, using effective media theories, from measurements made on a compressed disk with a porosity of 0.19. When plotted against the frequency, in the range 10^{-1}–3×10^6 Hz, Re ϵ for this disk was found to be virtually constant, and that the Re σ_M term could be fitted to Re $\sigma_M = \sigma_{dc} + D\omega^{0.9}$ (Ref. 25) with σ_{dc} being sensitive to how dry the BN in the disk was (and therefore also how dry the BN in the G-BN powder was). By pumping on the disks long enough the dc component became unmeasurable [i.e., $< 10^{-18}(\Omega\ \mathrm{m})^{-1}$ at 10^{-1} Hz]. D was independent of σ_{dc} and had a value of 9.0×10^{-16}. Unfortunately, the powders could not be pumped to lower values of σ_{dc} as this caused them to collapse.

Although the system is anisotropic,[7] if measurements are made in the axial (compression) and radial directions, it is probably still valid to use the Hashim-Strickman (HS) upper and lower bounds[26] for measurements made in the radial direction only. Therefore, Re σ_M and Im σ_M for ''bulk'' BN where determined using the upper bound, as the BN grains are obviously in contact at low volume fractions, which makes the system closer to one where the BN surrounds the air.[27] The bulk parameters are Re $\epsilon = 4.1$ and $D = 1.2 \times 10^{-15}$. As the critical volume fraction for the 55%G-45%BN system is 0.124, the upper limit for dilute systems was taken to be $\phi = 0.02$. At this volume fraction of G the volume fraction of BN was 0.0164 and of air 0.9636. Therefore the parameters determining σ_M for a system with 0.017 volume fraction of BN and 0.983 for air were calculated, again using the formula for the HS upper bound, which gave a Re $\epsilon = 1.03$ and a $D = 1.41.\times10^{-17}$ with σ_{dc} selected to fit the experimental results. The calculated Re σ_M at $\phi = 0.02$ is then used to evaluate the enhanced dielectric loss term, the percolation contribution and the combination of these, using Eqs. (5) and (15). These are all shown in Fig. 3. The computed value of Re σ_M for the air-BN insulator is not shown but lies below the enhanced curve by a factor of $s\phi/\phi_c$. The other values $s = 0.47$, $t = 4.8$, and $\sigma_C = 3126(\Omega\ \mathrm{m})^{-1}$, used to calculate these curves, have all been determined by dc percolation measurements[11,12] and σ_{dc} was chosen to match the curvature at low frequencies. The mean slopes of 1.05 for the squares and 1.09 for the crosses are lower than the value of $(1+4.8)/4.8 = 1.21$, as is predicted by Eq. (17). The discrepancy is explained by the comparatively large values of ϕ in the experimental results; in fact numerical solutions of Eq. (4) show that the $\omega^{1/(1+t)}$ behavior is flattening out for increasing ϕ as it has to attain the $\omega^{t/(s+t)}$ behavior for $\phi \to \phi_c$.

The only data that claim an ω^2 dependence for σ_M, $\phi < \phi_c$, is that of Benguigui.[21] However, there are problems with his data in a mixture of iron balls and glass beads. His sample contains only 10^5 particles (about 10^8 in the present experiments not even counting the air volume) and only 30 particles between the capacitor plates (nearly 300 plus air in the present experiments). Although Benguigui mentions the dc conductivity of the glass, it would appear that neither this nor the dielectric loss term in the glass is taken into account. The authors are also at a loss to explain how the very low frequency dispersion observed for Re $\epsilon(\omega)$ in an insulating

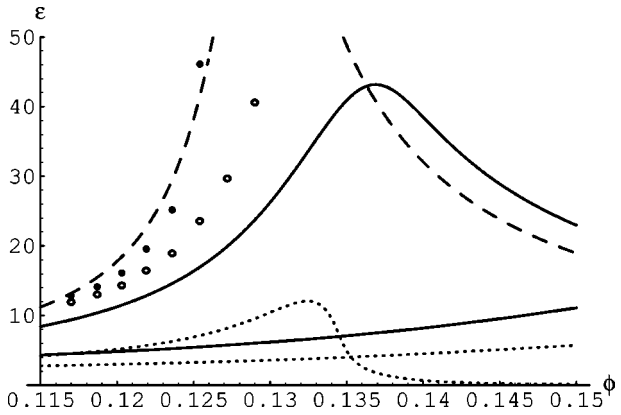

FIG. 4. Experimental values of Re ϵ for G-BN, plotted against ϕ, at 1 kHz (dots) and 1 MHz (circles). The nature and parameters for the theoretical curves are given in the text.

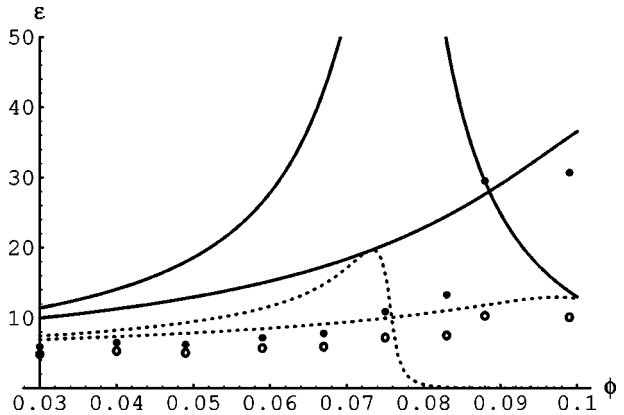

FIG. 5. Experimental values of Re ϵ for NbC coated grains, plotted against ϕ, at 1 kHz (dots) and 1 MHz (circles). The nature and parameters for the theoretical curves are given in the text.

20.0% iron balls sample (Fig. 2 in Ref. 21) can give a Re $\epsilon(\omega)\omega \sim$ Im $\sigma_M(\omega)$ which varies as ω^2 when plotted against the frequency (Fig. 8 in Ref. 21). Therefore we do not regard these experiments as definitive.

In Fig. 2 the dielectric results for the conducting samples are terminated at 1 kHz as for lower frequencies tan δ exceeds 10^3 and the dielectric spectrometer gives spurious results. However, the results at 1 kHz (a frequency commonly used in low frequency experiments to measure Re ϵ) clearly show that Re ϵ continues to increase with ϕ below and above ϕ_c. This is in sharp disagreement with the predictions given in Refs. 8–10, where it is claimed that Re ϵ should decrease as $(\phi-\phi_c)^{-s}$ for $\phi>\phi_c$.

The smooth behavior of Re ϵ as a function of ϕ passing and extending beyond ϕ_c has also recently been observed in carbon black-polyethylene composites[18] and a number of systems where various fine conducting powders are impregnated onto the surface of almost spherical insulator grains before the coated grains are compressed into a three-dimensional continuum.[19]. Therefore there is now strong experimental evidence that the second order term for $\phi>\phi_c$ given in Refs. 8–10 is in disagreement with experimental evidence. Their second-order percolation term also fails to vanish for $\phi\rightarrow 1$ in contrast to our result in Eq. (18).

However, Eqs. (1) and (4) show a Re ϵ that continues to increase above ϕ_c. Unfortunately, the agreement with the experimental results is qualitative, at best, if the parameters obtained from dc experiments are substituted into Eq. (4), as is shown in Figs. 4 and 5.

Figure 4 shows the experimental Re ϵ results at 1 kHz and 1 MHz, plotted against ϕ, for the G-BN powder. All theoretical curves, calculated from Eq. (4) are for $t=4.8$.[11] The solid curves are for $\sigma_C=3.1\times 10^3(\Omega\ \mathrm{m})^{-1}$,[7,11] Re $\epsilon=1.18$ (calculated ϕ_c value), $\phi_c=0.124$ and $s=0.96$. The upper solid curve is for 1 kHz and the lower one for 1 MHz. The dotted curves use the same parameters except that $s=0.6$. As the experimental results all lay above the theoretical curves, we display the dashed curve where σ_C has been changed to $3.1\times 10^5(\Omega\ \mathrm{m})^{-1}$. From this figure and the behavior of the theoretical plots it is apparent that the experimental results can be better fitted, if some or all of the above parameters are varied to get the best fit. In this case it would not be necessary to change ϕ_c from its dc value of 0.124 ± 0.001. As the dc conductivity changes by nine orders of magnitude between 0.120 and 0.130, one cannot argue that the incorrect ϕ_c has been identified.

Of the six powders that were coated onto the wax coated insulating grains, as previously described, only the nickel powder did not show an increasing Re ϵ above the dc value for ϕ_c, this was because the conductivity at and above ϕ_c was too high to measure Re ϵ.[19] This combined with the results for carbon black-polyethylene,[18] both as a function of ϕ, and ϕ_c (as a function of temperature) for fixed ϕ, show that this could well be the usual behavior for continuum systems. The reason that this has not been previously reported is probably due to the limitations of tan δ in the instruments previously used, and the fact that for $t\approx 2$ and large $\sigma_C/(\omega\epsilon_0\epsilon)$ ratios the solution of Eq. (4) is sharply peaked *just above* ϕ_c. To observe this difference accurate measurements of both the dc and the apparent ac value of ϕ_c (delayed peak in Re ϵ) would have had to be made. This has never been done except for the G-BN system, the coated grain system,[19] and to some extent the carbon black-polyethylene system.[18,28] In all the coated grain systems sharp changes in the dc curves of σ_M give unambiguous ϕ_c values.[19] With a poor conductor (magnetite) Re ϵ increases sharply near ϕ_c and then smoothly up to $3\phi_c$.[19]

Figure 5 shows the experimental results for Re ϵ for a system of insulating grains coated with NbC.[19]. All theoretical curves, calculated from Eq. (4), are for $t=4.8$. The solid curves are for $\sigma_C=7000(\Omega\ \mathrm{m})^{-1}$, Re $\epsilon=7.45$, $\phi_c=0.065$, and $s=0.8$. The upper solid curve is for 1 kHz and the lower one 1 MHz. The lower dotted curves are for the same parameters but $s=0.4$, which is the measured dc value. The low value for σ_C could be due to the resistance of the system being largely determined by contacts between the extremely hard and angular NbC grains. All the above parameters, except for $s=0.8$, are close to those obtained from the dc conductivity fit using Eq. (1). Except for the fact that the drop in ϵ for larger values of ϕ is not observed the results could be called qualitatively correct.

The curves selected do not show that the theoretical curves widen considerably as t is increased, i.e., the conductivity exponent plays a large role in determining Re ϵ. An explanation may be that as the conductivity of a percolating system above ϕ_c increases more slowly with ϕ for high t

values, this means that a smaller fraction of the conducting component is on the backbone of a system with a higher t value than a system with a lower t. This ''off the backbone'' conducting material then creates nearly conducting links between different sections of the backbone, which are broken by the insulating component. It would then be the effect of these inter *dead end* capacitances that continues to increase $\mathrm{Re}\,\epsilon$ above ϕ_c, until these capacitances are shorted out by an ever more conductive backbone.

V. SUMMARY AND CONCLUSIONS

In this paper we have shown analytically that Eq. (1), in conjunction with Eqs. (5) and (6), gives complex scaling functions for continuum percolation type systems with the following results:

(i) $\mathrm{Re}\,F_+(x_+)$ has zero slope for $x_+<1$ (first order term), and a slope of $t/(s+t)$ for $x_+>1$.

(ii) $\mathrm{Im}\,F_-(x_-)$ has slope unity for $x_-<1$ (first order term), and a slope of $t/(s+t)$ for $x_->1$.

(iii) A slope of $t/(s+t)$ for $\mathrm{Im}\,F_\pm$ and $\mathrm{Re}\,F_\pm$ for x_+ and $x_->1$.

Note that for x_+ and $x_->1$ one cannot clearly distinguish between first- and second-order terms. All of these limiting slopes agree with those given in Refs. 8–10. However, the $F_\pm$ in this paper are analytic functions with no unspecified constants. The functions $\mathrm{Re}\,F_+$ and $\mathrm{Im}\,F_-$ have been shown to continuously fit the first-order dispersion data for the G-BN systems over the whole range of values for $x_\pm$,[7] and $F_\pm$ the dc conductivity results for Al_xGe_{1-x}.[16]

The slopes for $\mathrm{Im}\,F_+$ and $\mathrm{Re}\,F_-$ for $x_\pm<1$ (second order terms) differ from those given in Refs. 8–10, which are based on the plausible assumptions made in Refs. 1–6. However, no definitive experimental verification of these two terms seems to exist and the new experimental work given here strongly favors the second order term for $\mathrm{Re}\,F_-$ given by Eqs. (1) and (5). The experimentally observed increases in $\mathrm{Re}\,\epsilon$ with ϕ above ϕ_c, some of which are given in Figs. 4 and 5, is completely incompatible with the percolation equations, as given in Refs. 8–10, but is qualitatively in agreement with Eq. (1) if the separately measured dc parameters are used. Better agreement between Eq. (1) and experiment could be obtained if best fit parameters were used.

From the above evidence Eq. (1) may well be a better description of the ac and dc conductivity (dielectric constant) of percolative type systems than the standard percolation equations given in Refs. 8–10. However, as Eq. (1) is a phenomenological equation its validity may need to be further tested by experiment as must the standard percolation equations.

ACKNOWLEDGMENTS

One of us (D.S.M.) would like to thank Professor B. I. Schlovskii for pointing out the necessity of taking the loss component of the insulating component into account and Professor A. K. Jonscher for a useful correspondence on low loss dielectrics.

[1] I. Webman, J. Jortner, and M. Cohen, Phys. Rev. B **11**, 2885 (1975).
[2] A. L. Efros and B. I. Shklovskii, Phys. Status Solidi B **76**, 475 (1976).
[3] J. P. Straley, J. Phys. C **9**, 783 (1976).
[4] J. P. Straley, J. Phys. C **10**, 3009 (1977).
[5] D. J. Bergman and Y. Imry, Phys. Rev. Lett. **39**, 1222 (1977).
[6] D. Stroud and D. J. Bergman, Phys. Rev. B **25**, 2061 (1981).
[7] Junjie Wu and D. S. McLachlan, Phys Rev B (to be published).
[8] J. P. Clerc, G. Girand, J. M. Langier, and J. M. Luck, Adv. Phys. **39**, 191 (1990).
[9] D. J. Bergman and D. Stroud, *Solid State Physics 46*, edited by H. Ehrenreich and D. Turnbull (Academic Press, San Diego, 1992), p. 147.
[10] Ce-Wen Nan, Prog. Mater. Sci. **37**, 1 (1993).
[11] J. Wu and D. S. McLachlan, Phys. Rev. B **56**, 1236 (1997)
[12] J. Wu, Ph.D thesis, University of the Witwatersrand, 1997.
[13] Y. Gefen, A. Aharony, and S. Alexander, Phys. Rev. Lett. **50**, 77 (1983).
[14] D. S. McLachlan and Michael B. Heaney (unpublished).
[15] C. Chiteme and D. S. McLachlan, in *Electrically Based Microstructure Characterization*, edited by R. A. Gerhardt, M. A. Alim, and S. R. Taylor (Materials Research Society, Pittsburgh, 1998).
[16] D. S. McLachlan, Physica B (to be published).
[17] D. S. McLachlan, J. Phys. C **20**, 865 (1987).
[18] D. S. McLachlan, M. Blaskiewics, and R. Newnham, J. Am. Ceram. Soc. **73**, 2187 (1990).
[19] R. Landauer, *Electrical Transport and Optical Properties of Inhomogeneous Media* edited by J. C. Garland and D. B. Tanner, AIP Conf. Proc. No. 40 (American Institute of Physics, 1978), p. 2.
[20] I. G. Chen and W. B. Johnson, J. Mat. Science **26**, 1565 (1991).
[21] L. Benguigui, J. Phys. (France) Lett. **46**, L1015 (1985).
[22] R. B. Laibowitz and Y. Gefen, Phys. Rev. Lett. **53**, 380 (1984)
[23] M. A. Van Dijk, G. Casteleijn, J. G. H. Joosten, and Y. K. Levine, J. Chem. Phys. **85**, 626 (1986).
[24] S. Bhattacharya, J. P. Stokes, M. W. Kim, and J. S. Huang, Phys. Rev. Lett. **55**, 1884 (1985).
[25] A. K. Jonscher, *Universal Relaxation Law* (Chelsea Dielectrics Press, London, 1996), Chap. 6.
[26] Z. Hashim and S. Shtrikman, J. Appl. Phys. **33**, 3123 (1962).
[27] D. S. McLachlan, in *Electrically Based Microstructure Characterization*, edited by R. A. Gerhardt, S. R. Taylor, and E. J. Garboczi, MRS Symp. Proc. No. 411 (Materials Research Society, Pittsburgh, 1996), p. 309.
[28] Michael B. Heaney, Phys. Rev. B **52**, 12 477 (1995).